Direct Synthesis of Porous Pure and Thiol-Functional Silica Spheres through the $S^+X^-I^+$ Assembly Pathway

Katsunori Kosuge,*,† Tatsuro Murakami,‡ Nobuyuki Kikukawa,† and Makoto Takemori†

Catalyst Development Group, Research Institute for Green Technology, National Institute of Advanced Industrial Science and Technology, 16-1 Onogawa, Tsukuba-shi, Ibaraki, 305-8569 Japan, and Mizusawa Industrial Chemicals, Ltd., 1-1 Mizusawa-cho, Nakajo-machi, Kitakanbara-gun, Niigata, 959-2638 Japan

Received February 11, 2003. Revised Manuscript Received June 3, 2003

Thiol-functional porous silica spheres with 100-μm mean diameter were synthesized in one quick step for ca. 60 min at room temperature using 1-alkylamine templating through the $S^+X^-I^+$ assembly pathway under an acidic condition. Thiol groups were introduced into materials while mesoporous silica spheres were prepared. SEM observation revealed that dodecylamine templating afforded a higher particle-shape quality than octylamine templating. Pore size and surface hydrophilicity of organic-functional silica spheres systematically decreased with increasing coverage of thiol groups on the pore surface, but the specific area was relatively constant. Thiol-functionalized silica spheres with 40% thiol loading resulted in microporous materials with hydrophobic pore surfaces for water vapor adsorption.

Introduction

Recent direct incorporation of organosiloxane moieties in mesostructured silica offers a promising route for preparation of inorganic−organic hybrid compounds.[1] Various organic-functionalized porous silicas have been synthesized through S^+I^-, S^0I^0, $S^+X^-I^+$, and N^0I^0 assembly processes.[1−4] Potential use of such derivatives depends critically on loading of accessible functional groups into the framework and also on macroscopic morphologies. Especially, those mesoporous spheres with micrometer size would be preferred because they are easily packed into existing reactors, columns, or fixed and fluidized-beds in various reaction systems. It is well-known that the thiol-functionalized porous silica, which is prepared through direct assembly pathways[5−7] as well as through grafting reactions of host materials,[8,9] has strong binding affinities for selected heavy metal ions such as Hg(II). Anchored thiol groups can be oxidized to provide sulfonic acid moeties for applications in solid acid catalysis.[7,10] However, few works have been published on totally well-controlled morphological products of thiol-functionalized porous silica spheres;[11] there have been few reports for such spheres functionalized with over 30% of silicon sites.[12]

On the other hand, since the first report of synthesis of M41S type mesoporous silica spheres by modifying Stöber's procedure,[13] in which aqueous ammonia or a strong base (NaOH, KOH, LiOH, RbOH, or TMAOH) was used as a catalyst to initiate hydrolytic polycondensation of tetraalkyl orthosilicate (TEOS), various porous silicas have been prepared.[14] Under an acidic aqueous solution, such types of silica hollow spheres were produced by controlled hydrolysis of TEOS in a stabilized emulsion of a biphasic system[15] including by evaporation-induced self-assembly process.[16] The diameter of almost all M41S type mesoporous silica was less

* To whom correspondence should be addressed. Telephone: +81-29-861-8492. Fax: +81-29-861-8459. E-mail: k.kosuge@aist.go.jp.
† National Institute of Advanced Industrial Science and Technology.
‡ Mizusawa Industrial Chemicals, Ltd.

(1) (a) Stein, A.; Melde, B. J.; Schroden, R. C. *Adv. Mater.* **2000**, *12*, 1403. (b) Sayari, A.; Hamoudi, S. *Chem. Mater.* **2001**, *13*, 3151.
(2) (a) Inagaki, S.; Guan, S.; Fukushima, Y.; Ohsuna, T.; Terasaki, O. *J. Am. Chem. Soc.* **1999**, *121*, 9611. (b) Guan, S.; Inagaki, S.; Ohsuna, T.; Terasaki, O. *J. Am. Chem. Soc.* **2000,** *122*, 5660. (c) Inagaki, S.; Guan, S.; Ohsuna, T.; Terasaki, O. *Nature* **2002**, *416*, 304.
(3) Melde, B. J.; Hollande, B. T.; Blanford, C. F.; Stein, A. *Chem. Mater.* **1999**, *11*, 3302.
(4) Asefa, T.; MacLachlan, M. J.; Coombs, N.; Ozin, G. A. *Nature* **1999**, *402*, 867.
(5) (a) Richer, R.; Mercier, L. *Chem. Commun.* **1998**, 1775. (b) Brown, J.; Richer, R.; Mercier, L. *Microporous Mesoporous Mater.* **2000**, *37*, 41.
(6) Brown, J.; Mercier, L.; Pinnavaia, T. J. *Chem. Commun.* **1999**, 69.
(7) Margolese, D.; Melero, J. A.; Christiansen, S. C.; Chmelka, B. F.; Stucky, G. D. *Chem. Mater.* **2000**, *12*, 2448.
(8) Feng, X.; Fryxell, G. E.; Wang, L.-Q.; Kim, A. Y.; Liu, J.; Kemner, K. M. *Science* **1997**, *276*, 923.
(9) (a) Mercier, L.; Pinnavaia, T. J. *Ad. Mater.* **1997**, *9*, 500. (b) Mercier, L.; Pinnavaia, T. J. *Environ. Sci. Technol.* **1998**, *32*, 2749.
(10) (a) Van Rhijin, W. M.; De Vos, D. E.; Sels, B. F.; Bossaert, W. D.; Jacob, P. A. *Chem. Commun.* **1998**, 317. (b) Lim, M. H.; Blanford, C. F.; Stein, A. *Chem. Mater.* **1998**, *10*, 467.
(11) (a) Bibby, A.; Mercier, L. *Chem. Mater.* **2002**, *14*, 1591. (b) Beaudet, L.; Hossain, K.-Z.; Mercier, L. *Chem. Mater.* **2003**, *15*, 327.
(12) Mori, Y.; Pinnavaia, T. J. *Chem. Mater.* **2001**, *13*, 2173.
(13) (a) Grün, M.; Lauer, I.; Unger, K. K. *Adv. Mater.* **1997**, *9*, 254. (b) Huo, Q.; Feng, J.; Schüth, F.; Stucky, G. D. *Chem. Mater.* **1997**, *9*, 14.
(14) For example: (a) Unger, K. K.; Kumar, D.; Grün, M.; Bückel, G.; Lüdtke, S.; Adam, T.; Schumacher, K.; Renker, S. *J. Chromatogr. A* **2000**, *892*, 47. (b) Fowler, C. E.; Khushalani, D.; Mann, S. *Chem. Commun.* **2001**, 2028. (c) Nooney, R. I.; Thirunavukkarasu, D.; Che, Y.; Josephs, R.; Ostafin, A. E. *Chem. Mater.* **2002**, *14*, 4721.
(15) For example: (a) Schacht, S.; Huo, Q.; Voigt-Martin, I. G.; Stucky, G. D.; Schüth, F. *Science* **1996**, *273*, 768. (b) Yang, H.; Vovk, G.; Coombs, N.; Sokolov, I.; Ozin, G. A. *J. Mater. Chem.* **1998**, *8*, 743. (c) Qi, L.; Ma, J.; Cheng, H.; Zhao, Z. *Chem. Mater.* **1998**, *10*, 1623. (d) Lin, H. P.; Cheng, Y. R.; Mou, C. Y. *Chem. Mater.* **1998**, *10*, 3772.
(16) Lu. Y.; Fan, H.; Stump, A.; Ward, T. L.; Rieker, T.; Brinker, C. J. *Nature* **1999**, *398*, 223.

10.1021/cm030225j CCC: $25.00
Published on Web 07/01/2003

than ca. 10 μm in all of the above syntheses; a relatively longer reaction time of 1−3 days or hydrothermal conditions were required to prepare those previous silica spheres. Furthermore, few works have been published for one-step preparation of M41S-type organic-functionalized porous silica spheres by modifying the above methods.[2a,17] Using a nonionic poly(ethylene oxide)-based surfactant, monodispersed MSU-X silica spheres ca. 10 μm in diameter,[18] and such thiol-functionalized mesoporous silica, microspheres were synthesized with relatively lower loading of thiol groups.[11] It has not been easy to prepare ordered silicas with high loading of organic moieties.[12,19] Highly thiol-functionalized products at loadings of 50−60%, while nonspherical particles, were synthesized by 1-alkylamine templating method of S°I° assembly pathway.[12]

We directly synthesized 30−40-μm mean-diameter Al-containing silica hard spheres under acidic conditions for ca. 1 h using 1-alkylamine as a structure-directing agent and TEOS as a silica source.[20] It was inferred that such mesoporous pure silica spheres would be produced, but this is not necessarily the case. Mesoporous spherical silicas have not been obtained as uniform monodispersed spheres with a higher quality of porous properties.[21] However, our simple, general procedure of a $S^+X^-I^+$ assembly pathway using 1-alkylamine as a structure-directing agent would be the first method to produce mesoporous hard spheres with definite diameter of several tens of micrometers.

Herein, we elucidate composition of reactant mixtures for monodispersed spherical mesoporous pure silica by rapid $S^+X^-I^+$ assembly process; then, we describe an analogous one-step synthesis of thiol-functional porous silica spheres of ca. 100-μm diameter with thiol loadings of 40%. Furthermore, our sorption property results for H_2O and C_6H_6 engender the important potential use of these thiol-functional porous silica spheres as volatile organic compound adsorbents.

Experimental Section

Material Synthesis. Purely inorganic mesostructural silica spheres were prepared by a modified procedure for Al-containing mesoporous silica spheres using 1-alkylamine as a structure-directing agent, and tetraethyl orthosilicate (TEOS) as a framework source. TEOS, 1-alkylamine, and ethanol were mixed for a definite time (3 min for octylamine, and 30 s for dodecylamine) with constant stirring rate; then, HCl aq. was rapidly added to this homogeneous solution with continued stirring for an additional 60 min. An improved Highflex Disperser HG92 (SMT Co., Ltd.) was used for our synthesis to control a lower definite stirring rate.

We investigated optimum synthetic conditions for uniform monodispersed spheres with higher quality of both morphological and porous properties at various reaction mixtures by octylamine templating at TEOS/octylamine (C8)/HCl/ethanol/H_2O (1.00: 0.17−0.70:0.06−0.17:0−2:37.7−74.4), and also by dodecylamine templating at TEOS/dodecylamine (C12)/HCl/ethanol/H_2O (1.00:0.29−0.65:0.004−0.007:0−2.54:37.7−40).

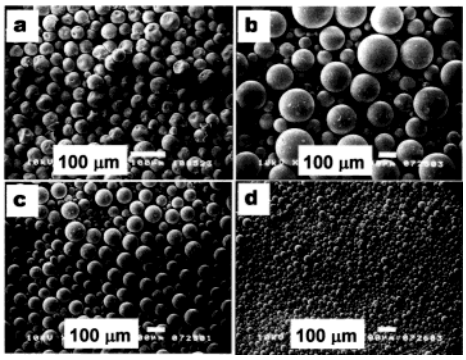

Figure 1. SEM images of purely inorganic mesostructural silica spheres obtained under optimum reactant composition of (a) TEOS/octylamine/HCl/ethanol/H_2O (1.00:0.34:0.068:1.94:38.0); and (b)−(d) TEOS/dodecylamine/HCl/ethanol/H_2O (1.00:0.35:0.004:0.88:38.0). Stirring rate is at (a) 600 rpm (sample 1 in Table 1), (b) 400 rpm, (c) 600 rpm (sample 3 in Table 1), and (d) 1000 rpm.

Organic-functionalized porous silica spheres were then synthesized in a similar manner using 3-mercaptopropyltrimethoxysilane [$(CH_3O)_3Si-(CH_2)_3SH$, MPTMS] as an organic-functional reagent together with TEOS. The initial mixing time of reactant solution was 3 min for each 1-alkylamine. Our spherical silicas were synthesized under reaction stoichiometry of TEOS+MPTMS/MPTMS/dodecylamine/HCl/ethanol/H_2O (1.00:x:0.35:0.004:0.90:39.0, where x = 0.10, 0.21, 0.40). Commercial chemicals were used with no additional purification. One quick step yielded solid products from a homogeneous reactant solution in the short time of ca. 60 min at room temperature.

Resultant products were collected by filtration then washed by ethanol several times and dried in air overnight. 1-alkylamine was removed by heat treatment in air for pure silica products, and by ultrasonic treatment for 0.5 g of as-synthesized thiol-functionalized products in 150 mL of ethanol with 4 mL of 5 M HCl aq. at 50 °C for 6 h. Samples were designated with SH−Si(x), where x shows the product's MPTMS loading.

Characterization. Powder X-ray diffraction (XRD) patterns were obtained with a Rigaku Rotaflex diffractometer equipped with a rotating anode and using Cu Kα radiation. Scanning electron microscopy (SEM) images were obtained on a JEOL5300. Particle size distribution was analyzed using a Coulter Multisizer III.

The N_2 sorption isotherms were obtained at −196 °C on a BELSORP 28 under continuous adsorption conditions. Prior to measurement, samples were heated at 200 °C for 2 h and finally outgassed to 10^{-3} Torr at room temperature; H_2O and C_6H_6 sorption isotherms were obtained at 25 °C on a BELSORP 18 where the samples were outgassed to 10^{-3} Torr at room temperature prior to the measurement. Especially in the case of water vapor sorption isotherms, the second, third, and fourth sorption isotherms were measured repeatedly in the same manner after another preevacuation at room temperature.

Solid-state MAS NMR spectra were recorded on a CMX 300 MHz NMR spectrometer using 7.5-mm zirconia rotors for ^{29}Si at 59.71 MHz. Sample spinning frequency was 3 kHz using 90° pulses at 600-s intervals with high power proton decoupling. The C, H, N, and S contents in the products were measured using an EA1110 CHNS−O analyzer (AMCO inc.).

Results and Discussion

Pure Silica Sphere. Figure 1a shows a SEM image of products obtained by the optimum C8 templating conditions in this work. Mesoporous pure silicas could not be obtained as uniform monodispersed spheres with

(17) Sayari, A.; Hamoudi, S.; Yang, Y.; Moudrakovski, I. L.; Ripmeester, J. R. *Chem. Mater.* **2000**, *12*, 3857.
(18) Boissière, C.; van der Lee, A.; El Mansouri, A.; Larbot, A.; Prouzet, E. *Chem. Commun.* **1999**, 2047.
(19) Kruk, M.; Asefa, T.; Jaroniec, M.; Ozin, G. A. *J. Am. Chem. Soc.* **2002**, *124*, 6383.
(20) Kosuge, K.; Singh, P. S. *Chem. Mater.* **2001**, *13*, 2476.
(21) Kosuge, K.; Singh, P. S. *Microporous Mesoporous Mater.* **2001**, *44*−*45*, 139.

Table 1. Physicochemical Properties of Mesoporous Pure Silica Spheres

sample	1-alkylamine carbon number	stirring rate (rpm)	surface area ($m^2\ g^{-1}$)	pore volume[a] ($mL\ g^{-1}$)	pore size[b] (nm)	particle size[c] (μm)
1	C8	600	1032	0.52	2.1	35
2	C12	400	854	0.92	3.6	74
3	C12	600	870	0.93	3.6	54
4	C12	800	875	0.89	3.5	32
5	C12	1000	869	0.91	3.5	22

[a] Framework pore volume as determined by t-plot analysis. [b] Pore diameter as estimated by BJH plots. [c] Particle size distribution was analyzed using a Coulter Multisizer III.

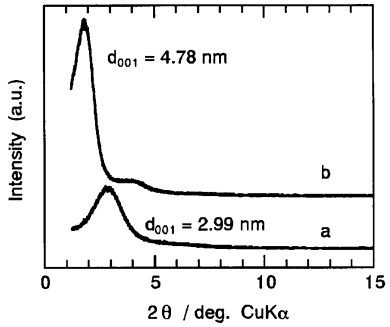

Figure 2. XRD patterns of representative calcined purely spherical silicas at 600 °C of (a) sample 1 and (b) sample 3 in Table 1.

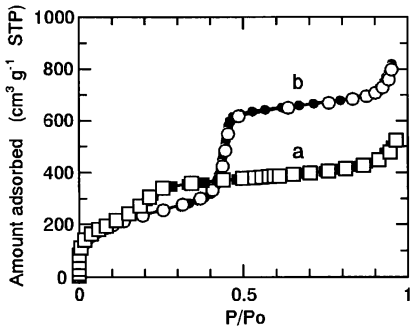

Figure 3. N_2 adsorption−desorption isotherms of products corresponding to (a) sample 1 and (b) sample 2 in Table 1. Filled symbols denote the desorption isotherm.

a higher morphological quality using octylamine as a structure-directing agent.

On the other hand, well-defined spherical mesoporous pure silicas with a definite diameter of several tens of micrometers were synthesized for a C12 templating as shown in Figure 1b and c. A higher stirring rate led to smaller spherical products (Figure 1d). Spheres synthesized using different stirring rates have mean particle sizes of 74 μm for 400 rpm, 54 μm for 600 rpm, 32 μm for 800 rpm, and 22 μm for 1000 rpm, whereas particle size distribution was found to broaden with decreasing stirring rate.

Corresponding X-ray diffraction (XRD) patterns and sorption isotherms of representative samples synthesized at optimum reactant compositions are shown in Figure 2 and Figure 3, respectively.

The XRD patterns of the spheres show an intense peak at a *d* spacing of ca. 3.2 nm for C8 and 5.2 nm for C12 along with a weak broad shoulder as shown in Figure 2. These properties are characteristic of mesoporous materials with a pore structure lacking long-range order such as those of the MSU[5a,11] and HMS[9,12] type samples.

Figure 3 shows N_2 sorption isotherms for corresponding silica spheres obtained by C8 and C12 templating.

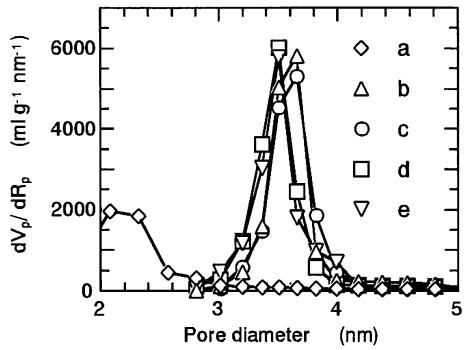

Figure 4. BJH pore size distribution curves of purely inorganic mesostructural silica spheres corresponding to (a)−(d) in Figure 1 along with (e) the sample obtained using dodecylamine at 800 rpm stirring rate.

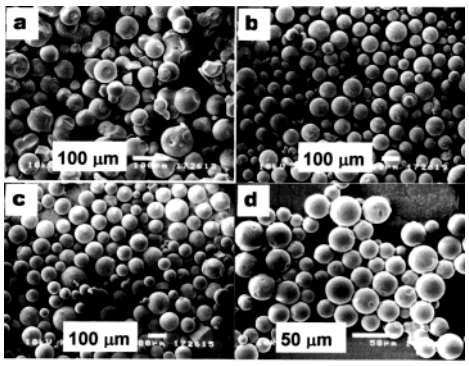

Figure 5. SEM images of thiol-functional porous silica spheres of (a) the product obtained by C8 templating, (b) SH−Si(9), (c) SH−Si(39), and (d) the samples corresponding to SH−Si(18) obtained at higher stirring speed of 1000 rpm.

Compared to isotherms of the sphere obtained by C8 templating, the adsorption step based on the filling of framework mesopores is remarkable for products for C12. There was no significant change in the shape of each isotherm of products synthesized at optimum reactant compositions irrespective of different stirring rates, indicating no significant effect of shear flow on porous properties; this is supported by BJH pore size distribution curves as shown in Figure 4. Mean pore diameters are ca. 2.1 nm for C8 and ca. 3.5−3.6 nm for C12. Steep adsorption increases are observed for both products at higher relative pressures that are attributed to additional textural mesopores among small constituent particles of spheres. Table 1 summarizes porous properties of pure silica spheres.

Thiol-Functional Porous Silica Spheres. Figure 5 shows SEM images of thiol-functional porous silica spheres obtained using C8 templating (Figure 4a) and C12 templating (Figure 4b−d). The mean diameter of thiol-functional porous silica spheres became a little larger than that of pure silica spheres. As expected in

Table 2. Physicochemical Properties of Thiol-Functional Porous Silica Spheres

sample	MPTMS in reactant (%)	MPTMS in product[a] (%)	surface area[b] ($m^2 g^{-1}$)	pore volume[c] (mL g^{-1})	pore size[d] (nm)	particle size[e] (μm)
SH−Si(9)	10	9	810	1.03	2.8	100
SH−Si(18)	20	18	847	0.78	2.1	100
SH−Si(39)	40	39	807	0.51		100

[a] Modified Si against total Si ($T^m/T^m + Q^n$) evaluated by ^{29}Si MAS NMR spectra. [b] Surface area was evaluated by t-plot analysis because sufficient linearity was not obtained on normal BET plots for products. [c] Framework pore volume as determined by t-plot analysis. [d] Pore diameter as estimated by BJH plots. [e] Particle size distribution was analyzed using a Coulter Multisizer III.

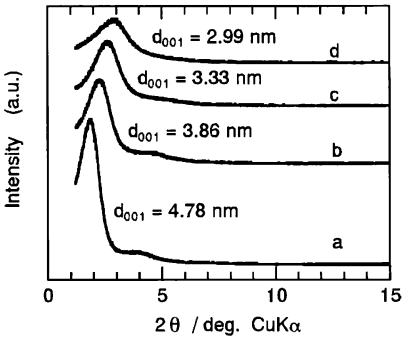

Figure 6. XRD patterns of thiol-functional porous silica spheres of (b) SH−Si(9), (c) SH−Si(18), and (d) SH−Si(39) together with (a) a porous silica sphere of sample 3 in Table 1 to indicate the effect on intensity and position of d001 peaks with organic functionalization.

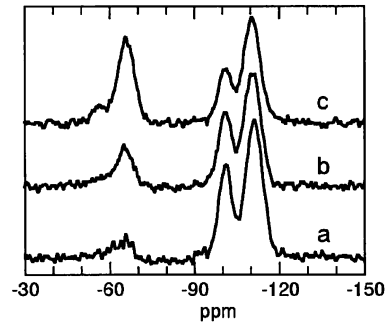

Figure 7. ^{29}Ni MAS NMR spectra of thiol-functional porous silica spheres of (a) SH−Si(9), (b) SH−Si(18), and (c) SH−Si(39).

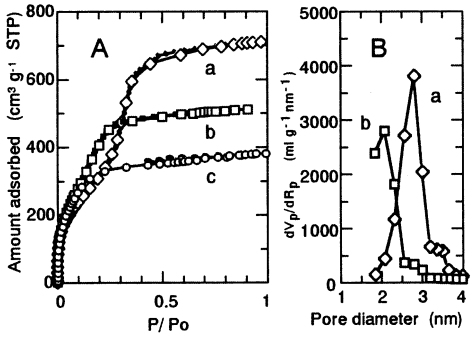

Figure 8. (A) N_2 adsorption−desorption isotherms of thiol-functional porous silica spheres of (a) SH−Si(9), (b) SH−Si-(18), and (c) SH−Si(39), and (B) corresponding BJH pore distribution curves. Filled symbols denote the desorption isotherm.

results for the product obtained by C8 templating (Figure 1a), we could not produce thiol-functional mesoporous silicas as uniform monodispersed spheres with a high quality of morphology using C8 templating (Figure 5a). On the other hand, Figure 5b and c shows that the thiol-functional samples for C12 are uniform monodispersed spheres with 100-μm mean diameter; their sizes are almost identical irrespective of the organic amount loaded.

Furthermore, a higher stirring rate at 1000 rpm led to smaller diameter of spherical products with 27 μm (Figure 5d), although there was little difference in loaded thiol amounts. On the other hand, such a stirring effect caused a slight decrease in mesoporosity of thiol-functional spheres, as shown in XRD patterns and N_2 sorption isotherms (Supporting Information). We could see only slight differences among N_2 sorption isotherms relative to stirring rate for the case of pure silica spheres. However, those differences did not lead to a remarkable change of pore surfaces properties, as shown in the respective sorption isotherms of H_2O and C_6H_6 (Supporting Information).

From morphological quality and the stirring effect on monodispersed spherical particles, our investigation hereafter addresses thiol-functional samples obtained by C12 templating at the definite stirring rate of 600 rpm.

Figure 6 shows XRD patterns of thiol-functional samples, indicating wormhole pore structures similar to those of nonfunctional pure silica spheres. The d_{100} reflections become weak and broad with increased amount of functional group along with a shift toward higher angles.

Figure 7 shows that ^{29}Si MAS NMR spectra of the functionalized products obtained by C12 templating denoted the presence of signals at −66 ppm (T^3, $(SiO)_3Si(CH_2)_3SH$) and −57 ppm (T^2, $(SiO)_2Si(OH)(CH_2)_3SH$) corresponding to the organosiloxane and −110 ppm (Q, ^{4} $Si(OSi)_4$) and −101 ppm (Q^3, $Si(OSi)_3(OH)$) based on the framework silica derived from hydrolyzed TEOS.[5,7,9,12] Existence of T^m signals and the increase of their intensity with increased functional group loading indicate that samples demonstrated incorporation of MPTMS within the silicate frameworks.[7] Comparing relative integral intensities of MPTMS signals with respect to total signal intensity ($T^m/T^m + Q^n$), we deduced that the amount of thiol groups incorporated in materials corresponded, within the limits of experimental uncertainty, to stoichiometry of the synthesis mixture (Table 2).

The N_2 adsorption−desorption isotherms shown in Figure 8a and corresponding BJH pore size distribution curve shown in Figure 8b reveal that surface and pore sizes of materials systematically decrease as a result of increased coverage of thiol groups on the pore surface; eventually, organic functionalization inside mesopores produces microporous materials. Unlike purely inorganic mesostructural silica spheres, additional textural mesopores are not observed for thiol-functional samples.

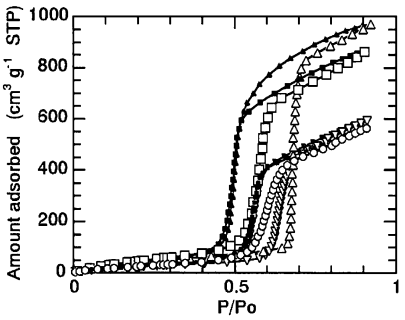

Figure 9. H_2O adsorption−desorption isotherms for the thiol-functional porous silica spheres of (△), (□) SH−Si(18) and of (▽), (○) SH−Si(39): △ and ▽ show first sorption isotherms; □ and ○ show second sorption isotherms. Filled symbols denote the desorption isotherm.

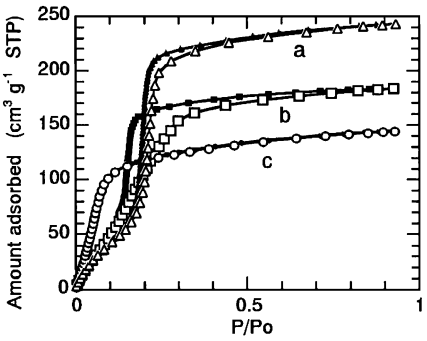

Figure 10. C_6H_6 adsorption−desorption isotherms of the thiol-functional porous silica spheres of (a) SH−Si(9), (b) SH−Si(18), and (c) SH−Si(39). Filled symbols denote the desorption isotherm.

Table 2 summarizes porous properties of thiol-functional silica spheres and MPTMS compositions.

Particle Formation. Suggested formation processes of organic-functional porous silica spheres are as follows.[20] A neutral S^0I^0 assembly was initially formed with a mixed solution of alkoxides and organic silicon (I^0) and 1-alkylamine (S^0) solution;[22] then, immediate nucleation of $S^+X^-I^+$ assembly was performed through addition of aq. HCl with a Coulombic interaction between charged species, protonated amine (S^+), coordinating anions of Cl^- (X^-), and the positively charged silica hybrid oligomer (I^+), including organic functional groups. As the alkyl chain carbon number increases, basicity on 1-alkylamine increases and the Coulombic is strong; hence, nucleation and growth of surfactant−inorganic $S^+X^-I^+$ assemblies occurred under more moderate synthetic conditions with relatively lower acidity when using dodecylamine as a template. Experimental results indicated that slight increase of the HCl amount in the reactant mixture for C12 templating produced agglomerated solids of spherical particles. Thus, relatively lower acidity in addition to ethanol as a cosolvent, which decrease the polarity of the solvent, would synergistically decrease the rate of nucleation and growth of mesostructured $S^+X^-I^+$ assemblies because of the slow TEOS hydrolysis.[23] Moreover, it has been pointed out that ethanol leads to formation of shorter self-assembled micelles because of lower polarity of the solvent.[24] Development of $S^+X^-I^+$ assemblies using C12 results in formation of smaller primary particles. Their growth should yield monodispersed spherical particles with better quality under a rapid one-step process. Furthermore, addition of MTPMS into TEOS might lead to their slower nucleation and growth as a result of slower hydrolysis. Consequently, this would result in enlarged particle diameter and no additional textural mesopores for thiol-functional spheres (Figure 8) compared with that of nonfunctional samples (Figure 3).

Sorption Properties. Figure 9 shows first and second sorption isotherms of water vapor on the thiol-functional spheres of SH−Si(18), and SH−Si(39). Both isotherms exhibit a type-V isotherm[25] that is characterized by a small-adsorbed H_2O amount at lower relative pressure, indicating a weak interaction between their pore surfaces and H_2O molecules. Steepness increases further for each sample because of capillary condensation of water vapor into pores that exist at higher P/Po. Furthermore, each sample shows distinct hysteresis in adsorption and desorption isotherms, which are smaller for second isotherms than for the first, indicating a decrease in hydrophobicity on pore surfaces after the first measurement. It should be noted that the vertical rise of the second adsorption isotherm for SH−Si(39) occurs at higher relative pressure at ca. P/Po = 0.6 than that at ca. P/Po = 0.5 for SH−Si(18). This behavior would be reversed if both samples had nearly similar pore surfaces with different pore sizes; capillary condensation of water vapor into smaller mesopores generally begins at lower relative pressure than it does larger ones.[26] Such characteristic features can be explained by the larger amount of silanol groups on the pore wall of SH−Si(18) than those of SH−Si(39). Furthermore, third and fourth isotherms are nearly superimposed upon the second one for SH−Si(39), suggesting that repetition of water vapor adsorption would not decrease hydrophobicity of the pore surfaces of SH−Si(39) and allow reversible sorption of water. These sorption behaviors indicate that the thiol-functional product of SH−Si(39) exhibited a remarkable hydrophobic pore surface due to relatively larger loading thiol groups that hindered water vapor access.

Figure 10 shows sorption isotherms on thiol-functional samples for C_6H_6 which are representative of harmful volatile organic compounds (VOCs). The C_6H_6 isotherms vary dramatically on coverage of thiol groups on the pore surface from type IV of the IUPAC classification for SH−Si(9) to type I for SH−Si(39). This indicates that the physisorption ability for C_6H_6 is systematically stronger with coverage of larger thiol groups on pore surfaces, indicating synergistic enhancement of adsorption affinity for C_6H_6 with decreasing pore size. These results as described above on sorption properties indicate that thiol-functionalized silica would be useful not only as a heavy metal ion adsorbent in aqueous

(22) Tanev, P. T.; Chibwe, M.; Pinnavaia, T. J. *Nature* **1994**, *368*, 321.
(23) Zhang, W.; Pauly, T. R.; Pinnavaia, T. J. *Chem. Mater.* **1997**, *9*, 2491.
(24) Lin, H. P.; Kao, C. P.; Mou, C. Y.; Liu, S. B. *J. Phys. Chem. B* **2000**, *104*, 7885.
(25) Sing, K. S. W.; Everett, D. H.; Haul, R. A. W.; Moscou, L.; Pierotti, R. A.; Rouquerol, J.; Siemienewska, T. *Pure Appl. Chem.* **1985**, *57*, 603.
(26) Naono, H.; Hakuman, M.; Tanaka, T.; Tamura, N.; Nakai, K. *J. Colloid Interface Sci.* **2000**, *225*, 411.

solutions,[5−9] but may also be useful as an adsorbent for VOCs under ambient conditions in gas phase.

Conclusions

Mesoporous silica hard spheres with 70-μm mean diameter were synthesized in one quick step for ca. 60 min at room temperature due to immediate formation of the $S^+X^-I^+$ assembly through the neutral S^0I^0 assembly in a homogeneous solution using dodecylamine templating. Thiol-functional porous silica spheres with 100-μm mean diameter also can be obtained directly by an analogous process in which functional groups are introduced into materials while mesoporous silica spheres are prepared. Mean diameter of both spheres decreased slightly with the higher rate, whereas shear fluid flow has little effect on spherical morphology and porous properties. Every calcined sphere has a disordered wormhole-like pore structure and high surface areas in excess of 800 m^2/g.

Physicochemical properties of thiol-functional silica spheres such as pore size and surface hydrophilicity systematically vary with loaded amount of thiol groups. Eventually, organic-functionalization inside the mesopores results in microporous materials with hydrophobic pore surfaces. Stabilization of hydrophobic properties on pore surfaces would be important to utilize the siliceous materials as adsorbents in the presence of water vapor. Therefore, our thiol-functional silica spheres with higher loading of thiol groups have implications for development of an advanced absorption and separation reaction system, where active carbons and zeolites are not effective in practical use, because they are easily packed into existing reactors, columns, or fixed beds.

Supporting Information Available: XRD patterns and sorption isotherms of N_2, H_2O, and C_6H_6; and porous properties listed in a table for samples obtained with different stirring rates (PDF). This material is available free of charge via the Internet at http://pubs.acs.org.

CM030225J